Weak dispersion and weak temperature dependence of angle-resolved photoemission for heavy-fermion systems

Ming-wen Xiao, Zheng-zhong Li, and Wang Xu
Department of Physics, Nanjing University, Nanjing 210093, People's Republic of China
(Received 5 December 2001; published 18 June 2002)

By extending the Kondo lattice model to include an exchange term between the *c* and *f* electrons on nearest-neighbor sites, we proposed an extended model that can be used to explain the weak dispersion and weak temperature behaviors of angle-resolved photoemission spectroscopies observed recently in heavy-fermion systems in the high-temperature range ($T \gg T_K$, T_K: the Kondo temperature). The extended model can not only describe the electronic coherence at $T \ll T_K$, but also yield an angle-resolved photoemission peak to the *f* electrons at $T \gg T_K$, with weak dispersion and weak temperature dependence.

DOI: 10.1103/PhysRevB.65.235122 PACS number(s): 79.60.−i, 71.27.+a, 75.20.Hr

I. INTRODUCTION

As well known, heavy-fermion systems manifest many unusual and intriguing properties,[1] such as a large Pauli susceptibility and specific heat as compared to ordinary metals, which indicate a huge effective electronic mass. Recently, angle-resolved photoemission spectroscopy (ARPES) experiments,[2–4] as a direct probe to the electronic states, revealed an anomalous property on single crytalline samples, i.e., there still exists a peak structure in the spectroscopy even when $T \gg T_{\mathrm{K}}$, where T_{K} stands for the Kondo temperature, the characteristic temperature of a heavy-fermion system. In particular, the peak shows weak temperature dependence, and is weakly dispersive: the dispersion is of the order of 20–35 meV whereas the width of the conduction band is typically a few eV, which means that the highly localized *f* electrons form a narrow itinerant band above T_{K}.

Usually, single crytalline heavy-fermion systems are modeled by the periodical Anderson model (PAM) or the Kondo lattice model (KLM), both of them can account for the electronic coherence present in these systems at low temperatures, $T \ll T_{\mathrm{K}}$.[5–7] For the PAM, theoretical studies through Monte Carlo method[8] and the noncrossing approximation for lattice[9] show that it can produce an ARPES peak to the *f* electrons at $T \gg T_{\mathrm{K}}$, and the peak is relatively weakly temperature dependent, but the spectral function for the *f* electrons, and also the corresponding ARPES are strongly dispersive.[8,9] For the KLM, it gives no dispersion to the *f* electrons at $T \gg T_{\mathrm{K}}$ because, as is well known, the *f* electrons are formed into independent localized magnetic moments at $T \gg T_{\mathrm{K}}$ within this model. This means that both the PAM and KLM are inadequate to describe the ARPES at $T \gg T_{\mathrm{K}}$, neither of them can give any exposition of the weak dispersion for the *f* electrons. Evidently, one must extend and complement those two models, or else resort to other models in order to interpret the two abnormal behaviors of the *f*-electron ARPES at $T \gg T_{\mathrm{K}}$.

In this paper, based on the Kondo lattice model, we shall try to develop a possible model for heavy-fermion systems, which is purposed to be able to provide not only a description of the low-temperature coherence but also of the *f*-electron ARPES peak at $T \gg T_{\mathrm{K}}$, including both its weak dispersion and weak temperature dependence. The rest of the paper is organized as follows: in Sec. II, we are going to extend the KLM to include a complementary exchange term between the *c* and *f* electrons on nearest-neighbor sites; in Sec. III, we aim at demonstrating that the extended Kondo model can still account for the electronic coherence at $T \ll T_{\mathrm{K}}$; in Sec. IV, we deal with the electronic states of the system at $T \gg T_{\mathrm{K}}$ within the extended model; in Sec. V, we explain the two abnormal behaviors of the *f*-electron ARPES at $T \gg T_{\mathrm{K}}$ with the results of Sec. IV; finally, in Sec. VI, we shall conclude our paper with a brief summary.

II. THE EXTENDED KONDO LATTICE MODEL

The Kondo lattice model reads as follows:[7]

$$H = \sum_{\mathbf{k},\sigma} \varepsilon_{\mathbf{k}} c^{\dagger}_{\mathbf{k},\sigma} c_{\mathbf{k},\sigma} - 2J \sum_{i} \mathbf{S}^{c}_{i} \cdot \mathbf{S}^{f}_{i}, \tag{1}$$

where $c_{\mathbf{k},\sigma}$ is the annihilation operator of the conduction-band electrons in the Bloch representation, and $\varepsilon_{\mathbf{k}}$ the corresponding energy; *J* is the intrasite exchange interaction, and $\mathbf{S}^{c}_{i}$ and $\mathbf{S}^{f}_{i}$ represent the spin operators on the *i*th site,

$$\mathbf{S}^{c}_{i} = \frac{1}{2}[c^{\dagger}_{i,\uparrow} c^{\dagger}_{i,\downarrow}] \vec{\tau} \begin{bmatrix} c_{i,\uparrow} \\ c_{i,\downarrow} \end{bmatrix}, \tag{2}$$

$$\mathbf{S}^{f}_{i} = \frac{1}{2}[f^{\dagger}_{i,\uparrow} f^{\dagger}_{i,\downarrow}] \vec{\tau} \begin{bmatrix} f_{i,\uparrow} \\ f_{i,\downarrow} \end{bmatrix}, \tag{3}$$

where $\vec{\tau}$ denotes the vector Pauli matrix, and $f_{i,\sigma}$ the annihilation operator of the localized electrons in the Wannier representation. Additionally, Eq. (1) must satisfy the constraints

$$\sum_{\sigma} f^{\dagger}_{i,\sigma} f_{i,\sigma} = 1 \tag{4}$$

on all sites.

As is well known, the KLM Hamiltonian of Eq. (1) is just a direct extension of the single-impurity Kondo model (SIKM),

$$H=\sum_{\mathbf{k},\sigma}\ \varepsilon_{\mathbf{k}}c^{\dagger}_{\mathbf{k},\sigma}c_{\mathbf{k},\sigma}-2J\mathbf{S}^{c}_{l}\cdot\mathbf{S}^{f}_{l}, \tag{5}$$

$$\sum_{\sigma}\ f^{\dagger}_{l,\sigma}f_{l,\sigma}=1 \tag{6}$$

by simply summing all the intrasite exchange terms present in the whole lattice, here l denotes the site index of the magnetic impurity. As pointed out in Sec. I, this extension is enough for describing the low-temperature coherence[5–7] occurring in heavy-fermion systems, but it is inadequate to account for the ARPES peak of the f electrons at $T\gg T_{\mathrm{K}}$. We think that the inadequacy results from the fact that such an extension is too simplified, viz., it neglects too many other exchange terms, especially the intersite ones. In the single magnetic impurity case, the exchange interaction between the c and f electrons can occur only on the same site, but for the lattice case, it can occur between the c and f electrons on different sites. To account for the ARPES peak of the f electrons, we should include the intersite exchange interaction.

To derive the exchange interaction between the c and f electrons on different sites, one can start from the electron-field operator, $\psi(\mathbf{r})$, as Kasuya did,[10]

$$\psi(\mathbf{r})=\sum_{\mathbf{k},\sigma}\ \varphi_{\mathbf{k}}(\mathbf{r})\,\eta_{\sigma}c_{\mathbf{k},\sigma}+\sum_{i,\sigma}\ w(\mathbf{r}-\mathbf{R}_i)\,\eta_{\sigma}f_{i,\sigma}, \tag{7}$$

where η_{σ} denotes the spin wave function, $\varphi_{\mathbf{k}}(\mathbf{r})$ and $w(\mathbf{r}-\mathbf{R}_i)$ the wave functions for the c and f electrons, respectively. In the single-impurity case, the second sum on the right-hand side of Eq. (7) reduces to a single piece: $w(\mathbf{r}-\mathbf{R}_l)\,\eta_{\sigma}f_{l,\sigma}$. With Eq. (7), the exchange interaction between the c and f electrons, H_{ex}, can be expressed as

$$H_{ex}=\sum_{i,j}\ \sum_{\mathbf{k},\mathbf{k}'}\ \sum_{\sigma,\sigma'}\ \langle\mathbf{k}i|v|j\mathbf{k}'\rangle c^{\dagger}_{\mathbf{k},\sigma}f^{\dagger}_{i,\sigma'}c_{\mathbf{k}',\sigma'}f_{j,\sigma}, \tag{8}$$

where

$$\langle\mathbf{k}i|v|j\mathbf{k}'\rangle=\int\int d\mathbf{r}d\mathbf{r}'\,\varphi^{\dagger}_{\mathbf{k}}(\mathbf{r})w^{\dagger}(\mathbf{r}'-\mathbf{R}_i)\times v(\mathbf{r}-\mathbf{r}')\varphi_{\mathbf{k}'}(\mathbf{r}')w(\mathbf{r}-\mathbf{R}_j) \tag{9}$$

with $v(\mathbf{r}-\mathbf{r}')$ representing the Coulomb interaction. By using the Bloch theorem

$$\varphi^{\dagger}_{\mathbf{k}}(\mathbf{r})=e^{-i\mathbf{k}\cdot\mathbf{R}_j}\varphi^{\dagger}_{\mathbf{k}}(\mathbf{r}-\mathbf{R}_j), \tag{10}$$

$$\varphi_{\mathbf{k}'}(\mathbf{r}')=e^{i\mathbf{k}'\cdot\mathbf{R}_i}\varphi_{\mathbf{k}'}(\mathbf{r}'-\mathbf{R}_i), \tag{11}$$

Eq. (9) can be formulated as

$$\langle\mathbf{k}i|v|j\mathbf{k}'\rangle=e^{i(\mathbf{k}'\cdot\mathbf{R}_i-\mathbf{k}\cdot\mathbf{R}_j)}\int\int d\mathbf{r}d\mathbf{r}'\,\varphi^{\dagger}_{\mathbf{k}}(\mathbf{r})w(\mathbf{r})\times v(\mathbf{r}-\mathbf{r}'-\mathbf{R}_i+\mathbf{R}_j)w^{\dagger}(\mathbf{r}')\varphi_{\mathbf{k}'}(\mathbf{r}'). \tag{12}$$

Expanding the Bloch wave functions $\varphi^{\dagger}_{\mathbf{k}}(\mathbf{r})$ and $\varphi_{\mathbf{k}'}(\mathbf{r}')$ into the Wannier functions $a^{\dagger}(\mathbf{r}-\mathbf{R}_m)$ and $a(\mathbf{r}'-\mathbf{R}_n)$,

$$\varphi^{\dagger}_{\mathbf{k}}(\mathbf{r})=\frac{1}{\sqrt{N}}\sum_{m}\ e^{-i\mathbf{k}\cdot\mathbf{R}_m}a^{\dagger}(\mathbf{r}-\mathbf{R}_m), \tag{13}$$

$$\varphi_{\mathbf{k}'}(\mathbf{r}')=\frac{1}{\sqrt{N}}\sum_{n}\ e^{i\mathbf{k}'\cdot\mathbf{R}_n}a(\mathbf{r}'-\mathbf{R}_n), \tag{14}$$

where N is the total number of the lattice sites, Eq. (12) can be further formulated as

$$\langle\mathbf{k}i|v|j\mathbf{k}'\rangle=\frac{1}{N}e^{i(\mathbf{k}'\cdot\mathbf{R}_i-\mathbf{k}\cdot\mathbf{R}_j)}\sum_{m}\ \sum_{n}\ e^{-i(\mathbf{k}\cdot\mathbf{R}_m-\mathbf{k}'\cdot\mathbf{R}_n)}\times\int\int d\mathbf{r}d\mathbf{r}'a^{\dagger}(\mathbf{r}-\mathbf{R}_m)w(\mathbf{r})\times v(\mathbf{r}-\mathbf{r}'-\mathbf{R}_i+\mathbf{R}_j)w^{\dagger}(r')a(\mathbf{r}'-\mathbf{R}_n). \tag{15}$$

The main contribution to the integral comes from the term with $\mathbf{R}_m=\mathbf{R}_n=0$,[10] and Eq. (15) can be approximated as

$$\langle\mathbf{k}i|v|j\mathbf{k}'\rangle=\frac{1}{N}e^{i(\mathbf{k}'\cdot\mathbf{R}_i-\mathbf{k}\cdot\mathbf{R}_j)}\int\int d\mathbf{r}d\mathbf{r}'a^{\dagger}(\mathbf{r})w(\mathbf{r})\times v(\mathbf{r}-\mathbf{r}'-\mathbf{R}_i+\mathbf{R}_j)w^{\dagger}(\mathbf{r}')a(\mathbf{r}'). \tag{16}$$

For the single-impurity case, $\mathbf{R}_i=\mathbf{R}_j=\mathbf{R}_l$, Eq. (8) reduces to

$$\begin{aligned}H_{ex}&=J\frac{1}{N}\sum_{\mathbf{k},\mathbf{k}'}\ \sum_{\sigma,\sigma'}\ e^{i(\mathbf{k}'-\mathbf{k})\cdot\mathbf{R}_l}c^{\dagger}_{\mathbf{k},\sigma}f^{\dagger}_{l,\sigma'}c_{\mathbf{k}',\sigma'}f_{l,\sigma}\\&=-J\sum_{\sigma,\sigma'}\ c^{\dagger}_{l,\sigma}c_{l,\sigma'}f^{\dagger}_{l,\sigma'}f_{l,\sigma}\\&=-2J\mathbf{S}^{c}_{l}\cdot\mathbf{S}^{f}_{l}-\frac{J}{2}\sum_{\sigma}\ c^{\dagger}_{l,\sigma}c_{l,\sigma},\end{aligned} \tag{17}$$

where we have used Eqs. (2)–(4), and

$$c_{l,\sigma}=\frac{1}{\sqrt{N}}\sum_{\mathbf{k}}\ e^{i\mathbf{k}\cdot\mathbf{R}_l}c_{\mathbf{k},\sigma}, \tag{18}$$

$$J=\int\int d\mathbf{r}d\mathbf{r}'a^{\dagger}(\mathbf{r})w(\mathbf{r})v(\mathbf{r}-\mathbf{r}')w^{\dagger}(\mathbf{r}')a(\mathbf{r}'). \tag{19}$$

The second term of H_{ex} is an unimportant potential scattering term, as usual, it can be omitted, and H_{ex} gives the second term of the SIKM of Eq. (5). Here, there can only exist the intrasite exchange between the c and f electrons.

In contrast to the single-impurity case, there can exist the intersite exchange between the c and f electrons in the case of periodical magnetic impurities, apart from the intrasite one. Correspondingly, the total exchange H_{ex} separates into two terms:

$$H_{ex}=-2J\sum_{i}\ \mathbf{S}^{c}_{i}\cdot\mathbf{S}^{f}_{i}-\sum_{i\neq j}\ \sum_{\sigma,\sigma'}\ J'_{i,j}c^{\dagger}_{i,\sigma}c_{j,\sigma'}f^{\dagger}_{j,\sigma'}f_{i,\sigma} \tag{20}$$

where

$$J'_{i,j}=\int\int d\mathbf{r}d\mathbf{r}'a^{\dagger}(\mathbf{r})w(\mathbf{r}) \times v(\mathbf{r}-\mathbf{r}'-\mathbf{R}_i+\mathbf{R}_j)w^{\dagger}(\mathbf{r}')a(\mathbf{r}'). \quad (21)$$

The first term of H_{ex} represents the intrasite exchange, which comes from the contribution of the components with $i=j$ in the sum over i and j of Eq. (8), and the second one the intersite exchange from the contribution of the components with $i\neq j$. The former will still exist even if there is only a single magnetic impurity alone in the system, but the latter will disappear if there is only one magnetic impurity. Again, an unimportant potential scattering term has been omitted in Eq. (20), as in the single-impurity case.

Clearly, the first term on the right-hand side of Eq. (20) is just a direct sum of all the intrasite terms present on each impurity site when compared with Eq. (17), and it yields the second term of the KLM Hamiltonian in Eq. (1). Physically, it describes the intrasite scattering between the c and f electrons, and cannot cause the f electrons to transit from site to site. On the contrary, the second term on the right-hand side of Eq. (20) can cause the f electrons to hop from site to site because it describes physically the intersite scattering between the c and f electrons. However, this term is excluded completely in the KLM Hamiltonian of Eq. (1); such exclusion leads to the result that the f electrons are all formed into independent local magnetic moments at $T\gg T_{\mathrm{K}}$ and gives no dispersion to the ARPES peak of the f electrons, which is in contradiction with the experiments,[2–4] as pointed out in Sec. I. We believe that this intersite scattering is responsible for the formation of the narrow itinerant band of the f electrons observed in the ARPES at $T\gg T_{\mathrm{K}}$, and it should be taken it into account and included in the Hamiltonian for the lattice case, which is the main idea for us to explain the ARPES of heavy-fermion systems in the this paper.

To determine the effect of this intersite scattering on the formation of the narrow f-electron itinerant band, we shall, for simplicity, keep only the exchange interaction from the nearest-neighbor sites because $J'_{i,j}$ decreases fast with the increasing of the distance $|\mathbf{R}_i-\mathbf{R}_j|$:

$$H=\sum_{\mathbf{k},\sigma}\varepsilon_{\mathbf{k}}c^{\dagger}_{\mathbf{k},\sigma}c_{\mathbf{k},\sigma}-2J\sum_i \mathbf{S}^c_i\cdot\mathbf{S}^f_i - J_1\sum_{\langle ij\rangle}\sum_{\sigma,\sigma'} c^{\dagger}_{i,\sigma}c_{j,\sigma'}f^{\dagger}_{j,\sigma'}f_{i,\sigma}, \quad (22)$$

where $\langle ij\rangle$ means the nearest-neighbor sites, and J_1 is the corresponding coupling strength, which is simplified as a constant for convenience, obviously, $|J_1|\ll|J|$. Except the last term, the above Hamiltonian is the same as the KLM, so we shall call it the extended Kondo lattice model (EKLM). In the following sections, we shall see that the J_1 term will cause the f electrons to form a narrow itinerant band at $T\gg T_{\mathrm{K}}$ and display a weak dispersion and weak temperature dependent ARPES. Besides, it will produce a renormalization to the electronic coherence at low temperatures, i.e., $T\ll T_{\mathrm{K}}$.

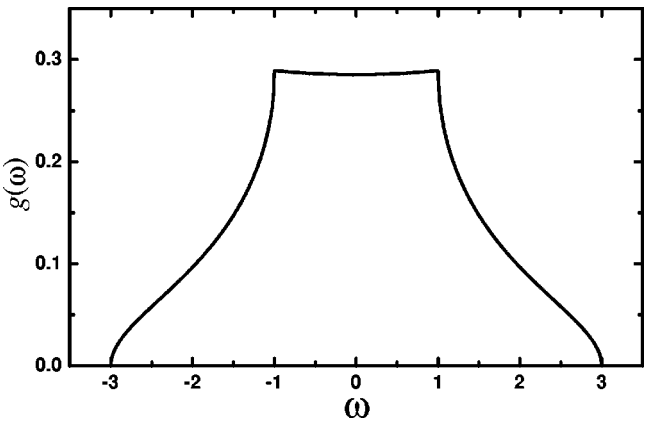

FIG. 1. The density of states of the undressed c electrons.

As usual, we shall introduce the chemical potential μ and the Lagrange multiplier ε_f to treat the conservation of particles and the constraint of Eq. (4),

$$H=\sum_{\mathbf{k},\sigma}\varepsilon_{\mathbf{k}}c^{\dagger}_{\mathbf{k},\sigma}c_{\mathbf{k},\sigma}-2J\sum_i \mathbf{S}^c_i\cdot\mathbf{S}^f_i - J_1\sum_{\langle ij\rangle}\sum_{\sigma,\sigma'} c^{\dagger}_{i,\sigma}c_{j,\sigma'}f^{\dagger}_{j,\sigma'}f_{i,\sigma}-\mu\left(\sum_{\mathbf{k},\sigma} c^{\dagger}_{\mathbf{k},\sigma}c_{\mathbf{k},\sigma} + \sum_{i,\sigma} f^{\dagger}_{i,\sigma}f_{i,\sigma}\right)+\sum_i \varepsilon_f\left(\sum_{\sigma} f^{\dagger}_{i,\sigma}f_{i,\sigma}-1\right), \quad (23)$$

which constitutes our working Hamiltonian. Accordingly, the parameters μ and ε_f are determined by the following equations:

$$N_t=\sum_{\mathbf{k},\sigma}\langle c^{\dagger}_{\mathbf{k},\sigma}c_{\mathbf{k},\sigma}\rangle+\sum_{i,\sigma}\langle f^{\dagger}_{i,\sigma}f_{i,\sigma}\rangle, \quad (24)$$

$$1=\frac{1}{N}\sum_{i,\sigma}\langle f^{\dagger}_{i,\sigma}f_{i,\sigma}\rangle, \quad (25)$$

where N_t is the total number of the electrons, and $\langle\cdots\rangle$ means the thermal average with respect to the working Hamiltonian. In the numerical calculations below, a tight-binding band of a simple cubic lattice will be supposed for the c electrons:

$$\varepsilon_{\mathbf{k}}=\varepsilon_0-t[\cos(k_xa)+\cos(k_ya)+\cos(k_za)], \quad (26)$$

where a denotes the lattice constant. The corresponding density of states

$$g(\omega)=-\frac{1}{\pi}\frac{1}{N}\sum_{\mathbf{k}}\mathrm{Im}\left(\frac{1}{\omega-\varepsilon_{\mathbf{k}}+i0^+}\right) \quad (27)$$

is shown in Fig. 1; here and hereafter, the c band parameters are chosen as $\varepsilon_0=0$, $t=1$, and $a=1$.

III. THE LOW-TEMPERATURE COHERENCE

For the sake of investigating the low-temperature electronic coherence, let us first reformulate the working Hamiltonian as

$$H=\sum_{\mathbf{k},\sigma}(\varepsilon_{\mathbf{k}}-J/2-\mu)c^{\dagger}_{\mathbf{k},\sigma}c_{\mathbf{k},\sigma}+\sum_{i,\sigma}(\varepsilon_f-\mu)f^{\dagger}_{i,\sigma}f_{i,\sigma}$$
$$+J\sum_{i}\sum_{\sigma,\sigma'}c^{\dagger}_{i,\sigma}f_{i,\sigma}f^{\dagger}_{i,\sigma'}c_{i,\sigma'}$$
$$+J_1\sum_{\langle ij\rangle}\sum_{\sigma,\sigma'}c^{\dagger}_{i,\sigma}f_{i,\sigma}f^{\dagger}_{j,\sigma'}c_{j,\sigma'}-N\varepsilon_f. \tag{28}$$

Henceforward, the energy constant $-J/2$ will be absorbed into the ε_0 of $\varepsilon_{\mathbf{k}}$ in Eq. (26).

Although the SIKM can be solved exactly,[11] the above model is hard to handle at present, just as the KLM. One must hence resort to approximation methods, of which the slave-boson mean-field (SBMF) approximation[5–7] is successful to describe the electronic coherence at low temperatures. Therefore, we shall adopt it here to study the low-temperature coherence. According to this method, one can treat the third and fourth terms on the right-hand side of Eq. (28) by introducing the SBMF parameter

$$b=\sum_{\sigma}\langle c^{\dagger}_{i,\sigma}f_{i,\sigma}\rangle=\sum_{\sigma}\langle f^{\dagger}_{i,\sigma}c_{i,\sigma}\rangle, \tag{29}$$

which leads to the mean-field Hamiltonian

$$H_{\mathrm{MF}}=\sum_{\mathbf{k},\sigma}(\varepsilon_{\mathbf{k}}-\mu)c^{\dagger}_{\mathbf{k},\sigma}c_{\mathbf{k},\sigma}+\sum_{\mathbf{k},\sigma}(\varepsilon_f-\mu)f^{\dagger}_{\mathbf{k},\sigma}f_{\mathbf{k},\sigma}$$
$$+\tilde{J}b\sum_{\mathbf{k},\sigma}(c^{\dagger}_{\mathbf{k},\sigma}f_{\mathbf{k},\sigma}+f^{\dagger}_{\mathbf{k},\sigma}c_{\mathbf{k},\sigma})-N(\varepsilon_f+\tilde{J}b^2), \tag{30}$$

where

$$\tilde{J}=J+6J_1, \tag{31}$$

$$f_{\mathbf{k},\sigma}=\frac{1}{\sqrt{N}}\sum_{l}e^{-i\mathbf{k}\cdot\mathbf{R}_l}f_{l,\sigma}. \tag{32}$$

Obviously, if $J_1=0$, $\tilde{J}$ reduces to J, and H_{MF} goes back to $H^{\mathrm{KLM}}_{\mathrm{MF}}$, the mean-field Hamiltonian for the Kondo lattice model

$$H^{\mathrm{KLM}}_{\mathrm{MF}}=\sum_{\mathbf{k},\sigma}(\varepsilon_{\mathbf{k}}-\mu)c^{\dagger}_{\mathbf{k},\sigma}c_{\mathbf{k},\sigma}+\sum_{\mathbf{k},\sigma}(\varepsilon_f-\mu)f^{\dagger}_{\mathbf{k},\sigma}f_{\mathbf{k},\sigma}$$
$$+Jb\sum_{\mathbf{k},\sigma}(c^{\dagger}_{\mathbf{k},\sigma}f_{\mathbf{k},\sigma}+f^{\dagger}_{\mathbf{k},\sigma}c_{\mathbf{k},\sigma})-N(\varepsilon_f+Jb^2), \tag{33}$$

which is the case studied in Refs. 6 and 7. Equation (30) indicates that the EKLM just renormalizes J into $\tilde{J}=J+6J_1$ in the mean-field approximation when compared with the KLM. Obviously, J_1 can strengthen or weaken $\tilde{J}$ if $J_1<0$ or $J_1>0$ $(J<0)$, since J is the intrasite exchange strength, whereas J_1 is the intersite exchange strength, it is believed that $|J_1|\ll|J|$. Thus, the renormalization is relatively small, and J_1 cannot reverse the sign of $\tilde{J}$, namely, $\tilde{J}$ keeps the same sign as J no matter whether J_1 is positive or negative: $\tilde{J}<0$. Because $\tilde{J}$ has the same sign as J, or they can be different merely in the magnitude, the physical results of H_{MF} at $T\ll T_{\mathrm{K}}$ are qualitatively the same as those of $H^{\mathrm{KLM}}_{\mathrm{MF}}$.

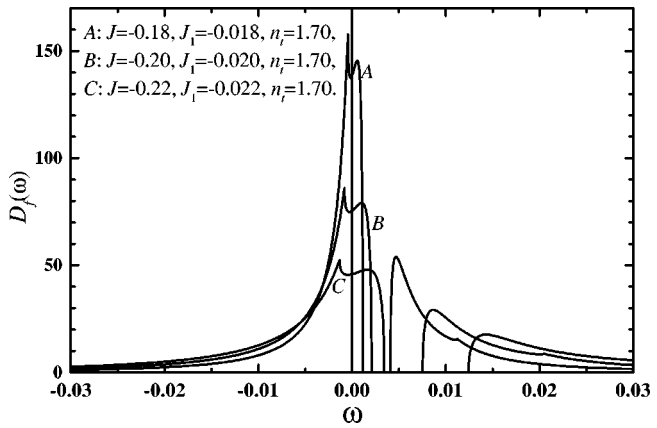

FIG. 2. The density of states of the f electrons at $T=0$ K.

As demonstrated in Refs. 6 and 7, $H^{\mathrm{KLM}}_{\mathrm{MF}}$ can account for the low-temperature coherence of heavy-fermion systems, therefore, H_{MF} can also account for the low-temperature coherence, i.e., the coherence is not broken but maintained within the extended Kondo lattice model, which is important to understand the properties of heavy-fermion systems at low temperatures. Equation (30) shows that the exchange interaction between the c and f electrons on nearest-neighbor sites can modify the electronic coherence at low temperatures through a renormalization.

A key manifestation of the coherence is that the f electrons are formed into a band at low temperatures, with a huge effective electronic mass, which can be seen straightforwardly from $D_f(\omega)$, the density of states of the f electrons

$$D_f(\omega)=-\frac{1}{\pi}\frac{1}{N}\sum_{\mathbf{k}}\mathrm{Im}\langle\langle f_{\mathbf{k},\sigma}|f^{\dagger}_{\mathbf{k},\sigma}\rangle\rangle_{\omega+i0^+}, \tag{34}$$

where $\langle\langle f_{\mathbf{k},\sigma}|f^{\dagger}_{\mathbf{k},\sigma}\rangle\rangle_z$ represents the f-electron Green's function obtained from Eq. (30). Its numerical results at $T=0$ K are shown in Fig. 2, where the chemical potential μ is taken as the origin of energy, and locates at the point of $\omega=0$. Figure 2 indicates that there arise two bands, for heavy-fermion metals, $n_t\lesssim 2$, where $n_t=N_t/N$ is the total number of the electrons per site, the chemical potential is positioned in the lower band. At the chemical potential, the density of states is huge, in comparison with the density of states of the bare c electrons in Fig. 1. As is well known, $m^*/m_e\simeq D_f(0)/g(0)$, where m^* and m_e are the effective f-electron and bare c-electron masses, respectively, this means that $m^*/m_e\gg 1$, namely, the f electrons get a huge effective mass.

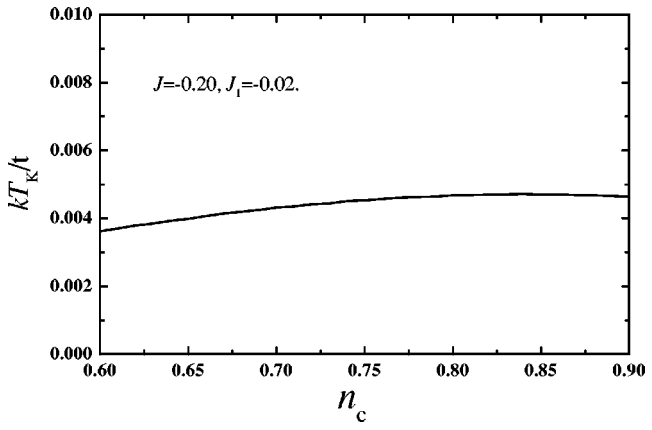

FIG. 3. The Kondo temperature versus the concentration of the c electrons.

Another important manifestation of the coherence is the onset of a characteristic energy scale, i.e., kT_{K}, where T_{K} is the so-called Kondo temperature, it is defined by[5–7]

$$kT_{\mathrm{K}}=\varepsilon_f-\mu, \tag{35}$$

where ε_f and μ take their values at $T=0$ K. The numerical results of T_{K} are shown in Fig. 3, where $n_c=n_t-1$ represents the number of the c electrons per site, it indicates that kT_{K}/t is rather small for a typical heavy-fermion system.

IV. THE ELECTRONIC STATES AT HIGH TEMPERATURES

Now, we turn to study the electronic states of the heavy-fermion system in the high-temperature range ($T\gg T_K$), we shall see that the intersite scattering between the c and f electrons can produce an essential influence on the f electrons and change radically their electronic states at high temperatures, though it just yields a renormalization to the low-temperature coherence and cannot revise qualitatively the electronic states of the system at low temperatures.

At high temperatures, the above slave-boson mean-field approximation being inappropriate, we must have recourse to other approximations. To do so, we would employ the method of the equation of motion for the Green's function,[12–15] and start from the working Hamiltonian of Eq. (23), which can be rewritten as

$$H=\sum_{\mathbf{k},\sigma}(\varepsilon_{\mathbf{k}}-\mu)c^{\dagger}_{\mathbf{k},\sigma}c_{\mathbf{k},\sigma}+\sum_{\mathbf{k},\sigma}(\varepsilon_f-\mu)f^{\dagger}_{\mathbf{k},\sigma}f_{\mathbf{k},\sigma}+H_1+H_2-N\varepsilon_f, \tag{36}$$

where

$$H_1=-2J\sum_i \mathbf{S}^c_i\cdot\mathbf{S}^f_i, \tag{37}$$

$$H_2=-J_1\sum_{\langle ij\rangle}\sum_{\sigma,\sigma'}c^{\dagger}_{i,\sigma}c_{j,\sigma'}f^{\dagger}_{j,\sigma'}f_{i,\sigma}. \tag{38}$$

With Eq. (36), the equation of motion for the Green's function $\langle\langle c_{\mathbf{k},\sigma}|c^{\dagger}_{\mathbf{k},\sigma}\rangle\rangle_z$ can be expressed as

$$\begin{aligned}z\langle\langle c_{\mathbf{k},\sigma}|c^{\dagger}_{\mathbf{k},\sigma}\rangle\rangle_z&=\langle\{c_{\mathbf{k},\sigma},c^{\dagger}_{\mathbf{k},\sigma}\}\rangle+\langle\langle[c_{\mathbf{k},\sigma},H]|c^{\dagger}_{\mathbf{k},\sigma}\rangle\rangle_z\\&=1+(\varepsilon_{\mathbf{k}}-\mu)\langle\langle c_{\mathbf{k},\sigma}|c^{\dagger}_{\mathbf{k},\sigma}\rangle\rangle_z\\&\quad+\langle\langle[c_{\mathbf{k},\sigma},H_1]|c^{\dagger}_{\mathbf{k},\sigma}\rangle\rangle_z\\&\quad+\langle\langle[c_{\mathbf{k},\sigma},H_2]|c^{\dagger}_{\mathbf{k},\sigma}\rangle\rangle_z,\end{aligned} \tag{39}$$

where $[A,B]$ and $\{A,B\}$ denote the commutator and anticommutator of A and B, respectively. Considering $|J_1|\ll|J|$, H_2 is much weaker than H_1, we shall thus continue $\langle\langle[c_{\mathbf{k},\sigma},H_1]|c^{\dagger}_{\mathbf{k},\sigma}\rangle\rangle_z$ forward with its equation of motion, but truncate $\langle\langle[c_{\mathbf{k},\sigma},H_2]|c^{\dagger}_{\mathbf{k},\sigma}\rangle\rangle_z$ with the factorization

$$\langle f^{\dagger}_{i,\sigma}f_{j,\sigma'}\rangle=r\,\delta_{\sigma,\sigma'}, \tag{40}$$

where $i\neq j$. For simplicity, we consider the paramagnetic case only. Evidently, $r=\langle f^{\dagger}_{i,\sigma}f_{j,\sigma}\rangle$ stands for the site-to-site hopping amplitude of the f electrons, which arises from the intersite exchange scattering with the c electrons. The factorization results in

$$\langle\langle[c_{\mathbf{k},\sigma},H_2]|c^{\dagger}_{\mathbf{k},\sigma}\rangle\rangle_z=\zeta_{\mathbf{k}}\langle\langle c_{\mathbf{k},\sigma}|c^{\dagger}_{\mathbf{k},\sigma}\rangle\rangle_z, \tag{41}$$

where

$$\zeta_{\mathbf{k}}=-2J_1r[\cos(k_xa)+\cos(k_ya)+\cos(k_za)], \tag{42}$$

that is to say $\langle\langle[c_{\mathbf{k},\sigma},H_2]|c^{\dagger}_{\mathbf{k},\sigma}\rangle\rangle_z$ has gone back to the initial Green's function $\langle\langle c_{\mathbf{k},\sigma}|c^{\dagger}_{\mathbf{k},\sigma}\rangle\rangle_z$. To continue $\langle\langle[c_{\mathbf{k},\sigma},H_1]|c^{\dagger}_{\mathbf{k},\sigma}\rangle\rangle_z$ forward, we first decompose it as

$$\langle\langle[c_{\mathbf{k},\sigma},H_1]|c^{\dagger}_{\mathbf{k},\sigma}\rangle\rangle_z=-\frac{J}{N}\sum_n\sum_{\mathbf{k}'}\sum_{\nu}e^{i(\mathbf{k}'-\mathbf{k})\cdot\mathbf{R}_n}\langle\langle\mathbf{S}^f_n\cdot\vec{\tau}_{\sigma\nu}c_{\mathbf{k}',\nu}|c^{\dagger}_{\mathbf{k},\sigma}\rangle\rangle_z, \tag{43}$$

and then handle $\langle\langle\mathbf{S}^f_n\cdot\vec{\tau}_{\sigma\nu}c_{\mathbf{k}',\nu}|c^{\dagger}_{\mathbf{k},\sigma}\rangle\rangle_z$ with its equation of motion

$$\begin{aligned}z\langle\langle\mathbf{S}^f_n\cdot\vec{\tau}_{\sigma\nu}c_{\mathbf{k}',\nu}|c^{\dagger}_{\mathbf{k},\sigma}\rangle\rangle_z&=\langle\{\mathbf{S}^f_n\cdot\vec{\tau}_{\sigma\nu}c_{\mathbf{k}',\nu},c^{\dagger}_{\mathbf{k},\sigma}\}\rangle+\langle\langle[\mathbf{S}^f_n\cdot\vec{\tau}_{\sigma\nu}c_{\mathbf{k}',\nu},H]|c^{\dagger}_{\mathbf{k},\sigma}\rangle\rangle_z\\&=\langle\mathbf{S}^f_n\rangle\cdot\vec{\tau}_{\sigma\nu}\delta_{\mathbf{k},\mathbf{k}'}\delta_{\sigma,\nu}+(\varepsilon_{\mathbf{k}'}-\mu)\langle\langle\mathbf{S}^f_n\cdot\vec{\tau}_{\sigma\nu}c_{\mathbf{k}',\nu},|c^{\dagger}_{\mathbf{k},\sigma}\rangle\rangle_z\\&\quad+\langle\langle[\mathbf{S}^f_n\cdot\vec{\tau}_{\sigma\nu}c_{\mathbf{k}',\nu},H_1]|c^{\dagger}_{\mathbf{k},\sigma}\rangle\rangle_z\\&\quad+\langle\langle[\mathbf{S}^f_n\cdot\vec{\tau}_{\sigma\nu}c_{\mathbf{k}',\nu},H_2]|c^{\dagger}_{\mathbf{k},\sigma}\rangle\rangle_z.\end{aligned} \tag{44}$$

As we have done with respect to $\langle\langle[c_{\mathbf{k},\sigma},H_2]|c^{\dagger}_{\mathbf{k},\sigma}\rangle\rangle_z$, we would also truncate $\langle\langle[\mathbf{S}^f_n\cdot\vec{\tau}_{\sigma\nu}c_{\mathbf{k}',\nu},H_2]|c^{\dagger}_{\mathbf{k},\sigma}\rangle\rangle_z$ with the factorization of Eq. (40),

$$\langle\langle[\mathbf{S}_n^f\cdot\vec{\tau}_{\sigma\nu}c_{\mathbf{k}',\nu},H_2]|c_{\mathbf{k},\sigma}^\dagger\rangle\rangle_z=\zeta_{\mathbf{k}'}\langle\langle\mathbf{S}_n^f\cdot\vec{\tau}_{\sigma\nu}c_{\mathbf{k}',\nu}|c_{\mathbf{k},\sigma}^\dagger\rangle\rangle_z, \tag{45}$$

it is thus closed into the left-hand side of Eq. (44). Regarding $\langle\langle[\mathbf{S}_n^f\cdot\vec{\tau}_{\sigma\nu}c_{\mathbf{k}',\nu},H_1]|c_{\mathbf{k},\sigma}^\dagger\rangle\rangle_z$, it breaks into two terms:

$$\begin{aligned}\langle\langle[\mathbf{S}_n^f\cdot\vec{\tau}_{\sigma\nu}c_{\mathbf{k}',\nu},H_1]|c_{\mathbf{k},\sigma}^\dagger\rangle\rangle_z&=\langle\langle[\mathbf{S}_n^f\cdot\vec{\tau}_{\sigma\nu},H_1]c_{\mathbf{k}',\nu}|c_{\mathbf{k},\sigma}^\dagger\rangle\rangle_z\\&\quad-\frac{J}{N}\sum_m\sum_{\mathbf{k}''}\sum_\gamma e^{i(\mathbf{k}''-\mathbf{k}')\cdot\mathbf{R}_m}\\&\quad\times\langle\langle\mathbf{S}_n^f\cdot\vec{\tau}_{\sigma\nu}\mathbf{S}_m^f\cdot\vec{\tau}_{\nu\gamma}c_{\mathbf{k}'',\gamma}|c_{\mathbf{k},\sigma}^\dagger\rangle\rangle_z.\end{aligned} \tag{46}$$

Using Eqs. (44)–(46), Eq. (43) becomes

$$\begin{aligned}&\langle\langle[c_{\mathbf{k},\sigma},H_1]|c_{\mathbf{k},\sigma}^\dagger\rangle\rangle_\omega\\&=\frac{J^2}{N^2}\sum_n\sum_{\mathbf{k}'}\sum_\nu\sum_m\sum_{\mathbf{k}''}\sum_\gamma e^{i[(\mathbf{k}'-\mathbf{k})\cdot\mathbf{R}_n+(\mathbf{k}''-\mathbf{k}')\cdot\mathbf{R}_m]}\\&\quad\times\frac{\langle\langle\mathbf{S}_n^f\cdot\vec{\tau}_{\sigma\nu}\mathbf{S}_m^f\cdot\vec{\tau}_{\nu\gamma}c_{\mathbf{k}'',\gamma}|c_{\mathbf{k},\sigma}^\dagger\rangle\rangle_z}{z-(\varepsilon_{\mathbf{k}'}+\zeta_{\mathbf{k}'}-\mu)}\\&\quad-\frac{J}{N}\sum_n\sum_{\mathbf{k}'}\sum_\nu e^{i(\mathbf{k}'-\mathbf{k})\cdot\mathbf{R}_n}\\&\quad\times\frac{\langle\langle[\mathbf{S}_n^f\cdot\vec{\tau}_{\sigma\nu},H_1]c_{\mathbf{k}',\nu}|c_{\mathbf{k},\sigma}^\dagger\rangle\rangle_z}{z-(\varepsilon_{\mathbf{k}'}+\zeta_{\mathbf{k}'}-\mu)},\end{aligned} \tag{47}$$

where we have used the fact that $\Sigma_n\langle\mathbf{S}_n^f\rangle=0$ in the paramagnetic case, which results in the contribution from the first term on the right-hand side of Eq. (44) becoming zero. Inserting it and Eq. (41) into Eq. (39), we get

$$\begin{aligned}&[z-(\varepsilon_{\mathbf{k}}+\zeta_{\mathbf{k}}-\mu)]\langle\langle c_{\mathbf{k},\sigma}|c_{\mathbf{k},\sigma}^\dagger\rangle\rangle_z\\&=1+\frac{J^2}{2N^2}\\&\quad\times\sum_\sigma\sum_n\sum_{\mathbf{k}'}\sum_\nu\sum_m\sum_{\mathbf{k}''}\sum_\gamma e^{i[(\mathbf{k}'-\mathbf{k})\cdot\mathbf{R}_n+(\mathbf{k}''-\mathbf{k}')\cdot\mathbf{R}_m]}\\&\quad\times\frac{\langle\langle\mathbf{S}_n^f\cdot\vec{\tau}_{\sigma\nu}\mathbf{S}_m^f\cdot\vec{\tau}_{\nu\gamma}c_{\mathbf{k}'',\gamma}|c_{\mathbf{k},\sigma}^\dagger\rangle\rangle_z}{z-(\varepsilon_{\mathbf{k}'}+\zeta_{\mathbf{k}'}-\mu)}\\&\quad-\frac{J}{2N}\sum_\sigma\sum_n\sum_{\mathbf{k}'}\sum_\nu e^{i(\mathbf{k}'-\mathbf{k})\cdot\mathbf{R}_n}\\&\quad\times\frac{\langle\langle[\mathbf{S}_n^f\cdot\vec{\tau}_{\sigma\nu},H_1]c_{\mathbf{k}',\nu}|c_{\mathbf{k},\sigma}^\dagger\rangle\rangle_z}{z-(\varepsilon_{\mathbf{k}'}+\zeta_{\mathbf{k}'}-\mu)},\end{aligned} \tag{48}$$

where the fact that $\langle\langle c_{\mathbf{k},\uparrow}|c_{\mathbf{k},\uparrow}^\dagger\rangle\rangle_\omega=\langle\langle c_{\mathbf{k},\downarrow}|c_{\mathbf{k},\downarrow}^\dagger\rangle\rangle_\omega$ in the paramagnetic case has been used.

For the second term on the right-hand side of Eq. (48), we first cut off the sum over $\mathbf{k}''$ with maintaining only the term of $\mathbf{k}''=\mathbf{k}$, and the sum over γ with of $\gamma=\sigma$, and then factorize $\Sigma_\nu\mathbf{S}_n^f\cdot\vec{\tau}_{\sigma\nu}\mathbf{S}_m^f\cdot\vec{\tau}_{\nu\sigma}$ out of the Green's function by including only the on-site spin correlation:[14,15] $\langle\Sigma_\nu\mathbf{S}_n^f\cdot\vec{\tau}_{\sigma\nu}\mathbf{S}_m^f\cdot\vec{\tau}_{\nu\sigma}\rangle=\delta_{m,n}\langle\mathbf{S}_n^f\cdot\mathbf{S}_n^f\rangle$, which results in

$$\begin{aligned}&\frac{J^2}{2N^2}\sum_\sigma\sum_n\sum_{\mathbf{k}'}\sum_\nu\sum_m\sum_{\mathbf{k}''}\sum_\gamma e^{i[(\mathbf{k}'-\mathbf{k})\cdot\mathbf{R}_n+(\mathbf{k}''-\mathbf{k}')\cdot\mathbf{R}_m]}\\&\quad\times\frac{\langle\langle\mathbf{S}_n^f\cdot\vec{\tau}_{\sigma\nu}\mathbf{S}_m^f\cdot\vec{\tau}_{\nu\gamma}c_{\mathbf{k}'',\gamma}|c_{\mathbf{k},\sigma}^\dagger\rangle\rangle_z}{z-(\varepsilon_{\mathbf{k}'}+\zeta_{\mathbf{k}'}-\mu)}\\&=J^2\left(\frac{1}{N}\sum_n\langle\mathbf{S}_n^f\cdot\mathbf{S}_n^f\rangle\right)\left(\frac{1}{N}\sum_{\mathbf{k}'}\frac{1}{z-(\varepsilon_{\mathbf{k}'}+\zeta_{\mathbf{k}'}-\mu)}\right)\\&\quad\times\langle\langle c_{\mathbf{k},\sigma}|c_{\mathbf{k},\sigma}^\dagger\rangle\rangle_z.\end{aligned} \tag{49}$$

Like the second term, we shall also deal with the third term by the cutoff approximation with $\mathbf{k}'=\mathbf{k}$ and $\nu=\sigma$,

$$\begin{aligned}&-\frac{J}{2N}\sum_\sigma\sum_n\sum_{\mathbf{k}'}\sum_\nu e^{i(\mathbf{k}'-\mathbf{k})\cdot\mathbf{R}_n}\\&\quad\times\frac{\langle\langle[\mathbf{S}_n^f\cdot\vec{\tau}_{\sigma\nu},H_1]c_{\mathbf{k}',\nu}|c_{\mathbf{k},\sigma}^\dagger\rangle\rangle_z}{z-(\varepsilon_{\mathbf{k}'}+\zeta_{\mathbf{k}'}-\mu)}\\&=-\frac{J}{2N}\sum_n\\&\quad\times\frac{\langle\langle[S_n^{fz},H_1]c_{\mathbf{k},\uparrow}|c_{\mathbf{k},\uparrow}^\dagger\rangle\rangle_z-\langle\langle[S_n^{fz},H_1]c_{\mathbf{k},\downarrow}|c_{\mathbf{k},\downarrow}^\dagger\rangle\rangle_z}{z-(\varepsilon_{\mathbf{k}'}+\zeta_{\mathbf{k}'}-\mu)}\\&=0,\end{aligned} \tag{50}$$

this is because $\langle\langle[S_n^{fz},H_1]c_{\mathbf{k},\uparrow}|c_{\mathbf{k},\uparrow}^\dagger\rangle\rangle_z=\langle\langle[S_n^{fz},H_1]c_{\mathbf{k},\downarrow}|c_{\mathbf{k},\downarrow}^\dagger\rangle\rangle_z$ in the paramagnetic case. Substituting Eqs. (49) and (50) into Eq. (48), we obtain

$$\begin{aligned}&[z-(\varepsilon_{\mathbf{k}}+\zeta_{\mathbf{k}}-\mu)]\langle\langle c_{\mathbf{k},\sigma}|c_{\mathbf{k},\sigma}^\dagger\rangle\rangle_z\\&=1+J^2\left(\frac{1}{N}\sum_n\langle\mathbf{S}_n^f\cdot\mathbf{S}_n^f\rangle\right)\\&\quad\times\left(\frac{1}{N}\sum_{\mathbf{k}'}\frac{1}{z-(\varepsilon_{\mathbf{k}'}+\zeta_{\mathbf{k}'}-\mu)}\right)\langle\langle c_{\mathbf{k},\sigma}|c_{\mathbf{k},\sigma}^\dagger\rangle\rangle_z.\end{aligned} \tag{51}$$

It can be written in a more compact form

$$\langle\langle c_{\mathbf{k},\sigma}|c_{\mathbf{k},\sigma}^\dagger\rangle\rangle_z=\frac{1}{z-(\varepsilon_{\mathbf{k}}+\zeta_{\mathbf{k}}-\mu)-\Sigma_c(z)}, \tag{52}$$

where $\zeta_{\mathbf{k}}$ is the energy renormalization arising from the site-to-site hoping due to the intersite exchange scattering, as indicated by Eq. (42) and $\Sigma_c(z)$ is the self-energy,

$$\Sigma_c(z)=J^2\left(\frac{1}{N}\sum_n\langle\mathbf{S}_n^f\cdot\mathbf{S}_n^f\rangle\right)\left(\frac{1}{N}\sum_{\mathbf{k}}\frac{1}{z-(\varepsilon_{\mathbf{k}}+\zeta_{\mathbf{k}}-\mu)}\right). \tag{53}$$

Apparently, it results from both the intrasite spin correlations and the intersite hoping of the f electrons, which are included in $\langle \mathbf{S}_n^f \cdot \mathbf{S}_n^f \rangle$ and $\zeta_{\mathbf{k}}$, respectively. Following Anderson,[16] we take only the imaginary part of $\Sigma_c(\omega + i0^+)$,

$$\Sigma_c(\omega + i0^+) = -i\pi J^2 \rho_c(0) \left(\frac{1}{N} \sum_n \langle \mathbf{S}_n^f \cdot \mathbf{S}_n^f \rangle \right) = -i\Gamma_c , \tag{54}$$

where

$$\rho_c(\omega) = -\frac{1}{\pi} \frac{1}{N} \sum_{\mathbf{k}} \mathrm{Im} \left(\frac{1}{\omega - (\varepsilon_{\mathbf{k}} + \zeta_{\mathbf{k}} - \mu) + i0^+} \right). \tag{55}$$

As a consequence

$$\langle\langle c_{\mathbf{k},\sigma} | c_{\mathbf{k},\sigma}^\dagger \rangle\rangle_{\omega + i0^+} = \frac{1}{\omega - (\varepsilon_{\mathbf{k}} + \zeta_{\mathbf{k}} - \mu) + i\Gamma_c}, \tag{56}$$

evidently, Γ_c stands for the damping of the c electrons.

By the same procedure as for $\langle\langle c_{\mathbf{k},\sigma} | c_{\mathbf{k},\sigma}^\dagger \rangle\rangle_{\omega + i0^+}$, we obtain

$$\langle\langle f_{\mathbf{k},\sigma} | f_{\mathbf{k},\sigma}^\dagger \rangle\rangle_{\omega + i0^+} = \frac{1}{\omega - (\varepsilon_f + \xi_{\mathbf{k}} - \mu) + i\Gamma_f}, \tag{57}$$

where

$$\xi_{\mathbf{k}} = -2J_1 s[\cos(k_x a) + \cos(k_y a) + \cos(k_z a)], \tag{58}$$

$$\Gamma_f = \pi J^2 \rho_f(0) \left(\frac{1}{N} \sum_n \langle \mathbf{S}_n^c \cdot \mathbf{S}_n^c \rangle \right) \tag{59}$$

with

$$s = \langle c_{i,\sigma}^\dagger c_{j,\sigma} \rangle, \tag{60}$$

$$\rho_f(\omega) = -\frac{1}{\pi} \frac{1}{N} \sum_{\mathbf{k}} \mathrm{Im} \left(\frac{1}{\omega - (\varepsilon_f + \xi_{\mathbf{k}} - \mu) + i0^+} \right). \tag{61}$$

By using Eqs. (56) and (57), the hopping amplitudes s and r in Eqs. (60) and (40) can be expressed in the case of simple cubic lattice as

$$s = -\frac{1}{6N} \sum_{\mathbf{k},\boldsymbol{\sigma}} \int_{-\infty}^{+\infty} \frac{d\omega}{\pi} f(\omega) [\cos(k_x a) + \cos(k_y a) + \cos(k_z a)] \mathrm{Im} \langle\langle c_{\mathbf{k},\sigma} | c_{\mathbf{k},\sigma}^\dagger \rangle\rangle_{\omega + i0^+}, \tag{62}$$

$$r = -\frac{1}{6N} \sum_{\mathbf{k},\boldsymbol{\sigma}} \int_{-\infty}^{+\infty} \frac{d\omega}{\pi} f(\omega) [\cos(k_x a) + \cos(k_y a) + \cos(k_z a)] \mathrm{Im} \langle\langle f_{\mathbf{k},\sigma} | f_{\mathbf{k},\sigma}^\dagger \rangle\rangle_{\omega + i0^+}, \tag{63}$$

where $f(\omega) = 1/(e^{\omega/kT} + 1)$ is the Fermi distribution function and k denotes the Boltzmann constant. With the same reason, Eqs. (24) and (25) can be formulated as

$$n_t = 1 - \frac{1}{N} \sum_{\mathbf{k},\boldsymbol{\sigma}} \int_{-\infty}^{+\infty} \frac{d\omega}{\pi} f(\omega) \mathrm{Im} \langle\langle c_{\mathbf{k},\sigma} | c_{\mathbf{k},\sigma}^\dagger \rangle\rangle_{\omega + i0^+}, \tag{64}$$

$$1 = -\frac{1}{N} \sum_{\mathbf{k},\boldsymbol{\sigma}} \int_{-\infty}^{+\infty} \frac{d\omega}{\pi} f(\omega) \mathrm{Im} \langle\langle f_{\mathbf{k},\sigma} | f_{\mathbf{k},\sigma}^\dagger \rangle\rangle_{\omega + i0^+}, \tag{65}$$

they are the equations about μ and ε_f.

As regards the on-site correlations $\langle \mathbf{S}_n^f \cdot \mathbf{S}_n^f \rangle$ and $\langle \mathbf{S}_n^c \cdot \mathbf{S}_n^c \rangle$, they can be calculated through Eqs. (2)–(4), with the result that

$$\frac{1}{N} \sum_n \langle \mathbf{S}_n^f \cdot \mathbf{S}_n^f \rangle = S(S+1), \tag{66}$$

$$\frac{1}{N} \sum_n \langle \mathbf{S}_n^c \cdot \mathbf{S}_n^c \rangle = \frac{3}{2} \frac{1}{N} \sum_{\mathbf{q}} \langle S^+(\mathbf{q}) S^-(\mathbf{q}) \rangle, \tag{67}$$

where $S = 1/2$ is the spin quantum number of the f electrons, and

$$S^+(\mathbf{q}) = \frac{1}{\sqrt{N}} \sum_{\mathbf{k}} c_{\mathbf{k}+\mathbf{q},\uparrow}^\dagger c_{\mathbf{k},\downarrow}, \tag{68}$$

$$S^-(\mathbf{q}) = \frac{1}{\sqrt{N}} \sum_{\mathbf{k}} c_{\mathbf{k},\downarrow}^\dagger c_{\mathbf{k}+\mathbf{q},\uparrow}, \tag{69}$$

the spin-density operators of the c electrons. With the help of the fluctuation-dissipation theorem,[12] $\langle S^+(\mathbf{q}) S^-(\mathbf{q}) \rangle$ can be represented by the Green's function $\langle\langle S^-(\mathbf{q}) | S^+(\mathbf{q}) \rangle\rangle_{\omega + i0^+}$,

$$\langle S^+(\mathbf{q}) S^-(\mathbf{q}) \rangle = -\int \frac{d\omega}{\pi} b(\omega) \mathrm{Im} \langle\langle S^-(\mathbf{q}) | S^+(\mathbf{q}) \rangle\rangle_{\omega + i0^+}, \tag{70}$$

where $b(\omega) = 1/(e^{\omega/kT} - 1)$ is the Bose distribution function. Physically, the Green's function $\langle\langle S^-(\mathbf{q}) | S^+(\mathbf{q}) \rangle\rangle_{\omega + i0^+}$ describes the spin fluctuation of the c electrons. If there is no interaction, i.e., $J = J_1 = 0$, it can be decoupled as

$$\begin{aligned} &\langle\langle S^-(\mathbf{q}) | S^+(\mathbf{q}) \rangle\rangle_{\omega + i0^+} \\ &= -\frac{1}{N} \sum_{\mathbf{k}} \int \frac{d\omega'}{\pi} [\langle\langle c_{\mathbf{k}+\mathbf{q},\uparrow} | c_{\mathbf{k}+\mathbf{q},\uparrow}^\dagger \rangle\rangle_{\omega + \omega' + i0^+}^{(0)} \\ &\quad \times \mathrm{Im} \langle\langle c_{\mathbf{k},\downarrow} | c_{\mathbf{k},\downarrow}^\dagger \rangle\rangle_{\omega' + 0^+}^{(0)} + \langle\langle c_{\mathbf{k},\downarrow} | c_{\mathbf{k},\downarrow}^\dagger \rangle\rangle_{\omega' - \omega + i0^+}^{(0)} \\ &\quad \times \mathrm{Im} \langle\langle c_{\mathbf{k}+\mathbf{q},\uparrow} | c_{\mathbf{k}+\mathbf{q},\uparrow}^\dagger \rangle\rangle_{\omega' + i0^+}^{(0)}] f(\omega'), \end{aligned} \tag{71}$$

where $\langle\langle c_{\mathbf{k},\sigma} | c_{\mathbf{k},\sigma}^\dagger \rangle\rangle_{\omega + i0^+}^{(0)}$ represents the Green's functions of the undressed c electrons. Considering that J and J_1 are both much less than the bandwidth of the undressed c electrons, they have very small influences on the of the c electrons. As a consequence, we shall still decouple $\langle\langle S^-(\mathbf{q}) | S^+(\mathbf{q}) \rangle\rangle_{\omega + i0^+}$ as in Eq. (71) under the interactions of J and J_1, but renormalize the undressed Green's functions into the corresponding dressed ones,

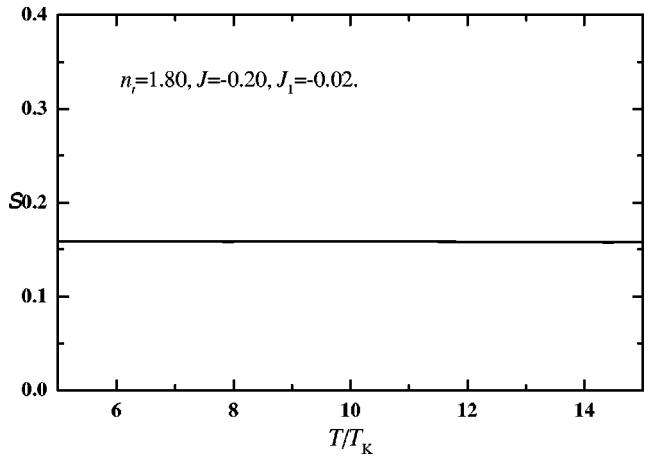

FIG. 4. The temperature dependence of the *c*-electron hopping amplitude.

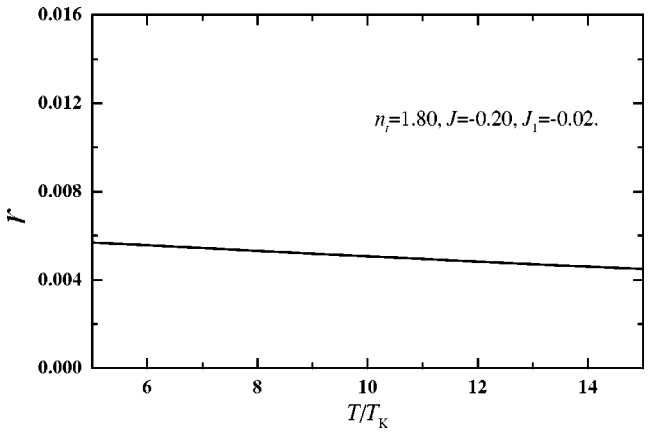

FIG. 5. The temperature dependence of the *f*-electron hopping amplitude.

$$\langle\langle S^-(\mathbf{q})|S^+(\mathbf{q})\rangle\rangle_{\omega+i0^+}$$
$$=-\frac{1}{N}\sum_{\mathbf{k}}\int\frac{d\omega'}{\pi}[\langle\langle c_{\mathbf{k}+\mathbf{q},\uparrow}|c^\dagger_{\mathbf{k}+\mathbf{q},\uparrow}\rangle\rangle_{\omega+\omega'+i0^+}$$
$$\times\mathrm{Im}\langle\langle c_{\mathbf{k},\downarrow}|c^\dagger_{\mathbf{k},\downarrow}\rangle\rangle_{\omega'+0^+}+\langle\langle c_{\mathbf{k},\downarrow}|c^\dagger_{\mathbf{k},\downarrow}\rangle\rangle_{\omega'-\omega+i0^+}$$
$$\times\mathrm{Im}\langle\langle c_{\mathbf{k}+\mathbf{q},\uparrow}|c^\dagger_{\mathbf{k}+\mathbf{q},\uparrow}\rangle\rangle_{\omega'+i0^+}]f(\omega'). \quad (72)$$

As a result of Eqs. (67), (70), and (72), we get

$$\frac{1}{N}\sum_n\langle\mathbf{S}^c_n\cdot\mathbf{S}^c_n\rangle$$
$$=\frac{3}{2}\int_{-\infty}^{+\infty}\frac{d\omega}{\pi}\int_{-\infty}^{+\infty}\frac{d\omega'}{\pi}b(\omega)[f(\omega')$$
$$+f(\omega'+\omega)]\left(\frac{1}{N}\sum_{\mathbf{k}}\mathrm{Im}\langle\langle c_{\mathbf{k},\downarrow}|c^\dagger_{\mathbf{k},\downarrow}\rangle\rangle_{\omega'+i0^+}\right)$$
$$\times\left(\frac{1}{N}\sum_{\mathbf{q}}\mathrm{Im}\langle\langle c_{\mathbf{q},\uparrow}|c^\dagger_{\mathbf{q},\uparrow}\rangle\rangle_{\omega'+\omega+i0^+}\right). \quad (73)$$

The discussions up to now show that Eqs. (56), (57), (62)–(65), and (73) constitute a closed set of equations of the self-consistent Hartree-Fock approximation (SCHFA), they are the basic equations for us to describe the electronic states of the *c* and *f* electrons at $T\gg T_K$ within the extended Kondo lattice model. If one likes to go beyond the SCHFA, he can further employ the parquet approximation due to Abrikosov[13] to include the effects of higher orders, which are less important and neglected here. The numerical results of *s* and *r* are shown in Figs. 4 and 5, respectively, clearly, they are both weak-temperature dependent.

Equations (57), (58), and (60) indicate that the site-to-site hoping due to the intersite exchange scattering produces an *f*-electron band with a dispersion of $\varepsilon_f+\xi_{\mathbf{k}}=\varepsilon_f-2J_1s[\cos(k_xa)+\cos(k_ya)+\cos(k_za)]$, the width of this band being proportional to J_1s. Because J_1 is much less than the bandwidth of the *c* electrons and $s\ll 1$ as shown in Fig. 4, the bandwidth of the *f* electrons is much less than that of the *c* electrons. In other words, the *f* electrons are formed into a narrow itinerant band under the intersite exchange scattering between the *f* and *c* electrons within the EKLM. On the contrary, if $J_1=0$ as in the KLM, the $\xi_{\mathbf{k}}$ will become zero, and the *f* electrons are formed into independent local magnetic moments with the energy level being at ε_f. That is the reason why we extend the KLM into the EKLM.

On the other hand, considering that the *c*-electron bandwidth is of the order of several eV, the *c* electronic state will depend on temperature weakly. As a result, the hopping amplitude $s=\langle c^\dagger_{i,\sigma}c_{j,\sigma}\rangle$ and the local spin correlation $\langle\mathbf{S}^c_n\cdot\mathbf{S}^c_n\rangle$ will vary rather slowly with the varying of temperature, it induces that both $\xi_{\mathbf{k}}\propto J_1s$ and $\Gamma_f\propto\langle\mathbf{S}^c_n\cdot\mathbf{S}^c_n\rangle$ change slowly with temperature, and so does the *f* Green's function $\langle\langle f_{\mathbf{k},\sigma}|f^\dagger_{\mathbf{k},\sigma}\rangle\rangle_{\omega+i0^+}$. Therefore, the *f* electronic state will be weakly temperature dependent within the EKLM.

These two features can be illustrated clearly by $\mathcal{A}_f(\mathbf{k},\omega)$, the spectral functions of the *f* electrons,

$$\mathcal{A}_f(\mathbf{k},\omega)=-\mathrm{Im}\langle\langle f_{\mathbf{k},\sigma}|f^\dagger_{\mathbf{k},\sigma}\rangle\rangle_{\omega+i0^+}, \quad (74)$$

which are shown, respectively, in Figs. 6 and 7. In Fig. 6, the shift of the peak is about 40 meV if the bandwidth of the bare *c* electrons is taken to be 6 eV, which means that the

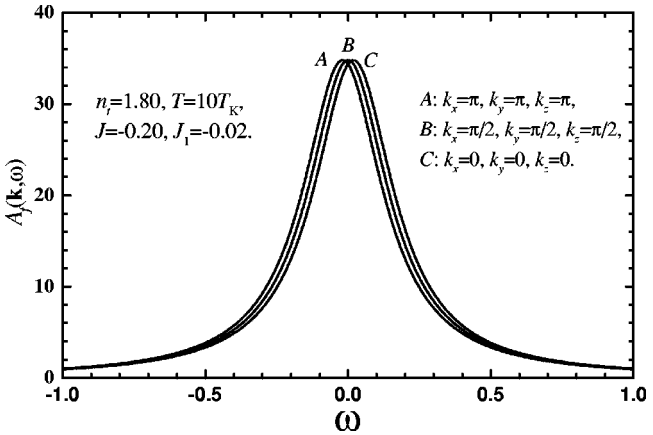

FIG. 6. The dispersion of the *f*-electron spectral function.

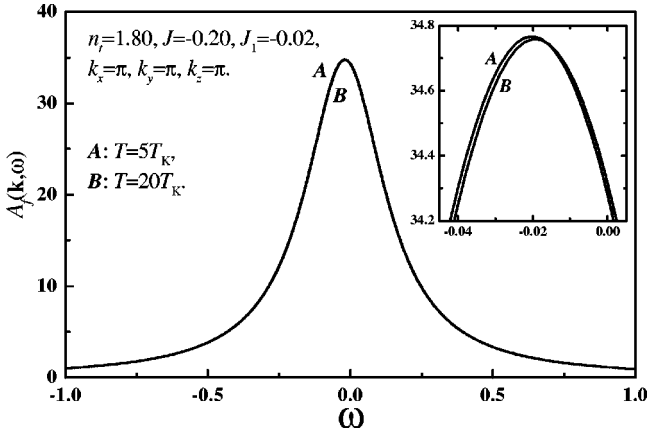

FIG. 7. The temperature dependence of the *f*-electron spectral function.

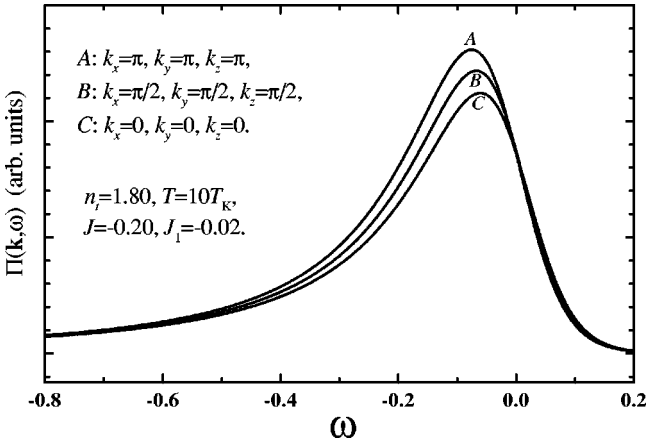

FIG. 8. The dispersion of the *f*-electron ARPES.

f-electron band is weakly dispersive. Compared with Refs. 8 and 9, Fig. 6 demonstrates that the *f* electrons within the EKLM is far less dispersive than within the PAM. The inset in Fig. 7 is an enlarged view, which indicates that the spectral function is nearly independent of temperature. Obviously, the numerical results are in accordance with the above qualitative analyses.

In sum, the *f*-electron state is both of weak dispersion and of weak temperature dependence at $T \gg T_K$ within the framework of the extended Kondo lattice model.

V. THE ARPES OF THE *F* ELECTRONS AT $T \gg T_K$

For the *f* electrons in the heavy-fermion system, which are strongly correlated, as proved in Refs. 17–20, their ARPES contains two parts: the elastic part and the inelastic part. The former contributes a peak to the ARPES, which gives the dispersion information of the electrons, but the latter contributes a background, which is irrelevant with the dispersion. As we are mainly concerned with the properties of the peak here, we shall consider only the elastic part of the ARPES, which is described by the differential cross section $\Pi(\mathbf{k},\omega)$,[17–20]

$$\Pi(\mathbf{k},\omega) \propto \mathcal{A}_f(\mathbf{k},\omega) f(\omega)$$

$$\propto \frac{\Gamma_f}{[\omega-(\varepsilon_f+\xi_{\mathbf{k}}-\mu)]^2+\Gamma_f^2} f(\omega) \tag{75}$$

$$\propto \frac{\Gamma_f}{[\omega'-(\varepsilon_f+\xi_{\mathbf{k}})]^2+\Gamma_f^2} f(\omega'-\mu), \tag{76}$$

where $\omega'=\omega+\mu$, and we take the Fermi level μ as the origin of the energy from now on. Clearly, the first factor on the right-hand side represents a Lorentzian peak with a center at $\varepsilon_f+\xi_{\mathbf{k}}$ and a half-width of Γ_f, and the second one a Fermi profile. Equation (76) indicates that the shift of the ARPES peak with the variation of $\mathbf{k}$ reflects the dispersion of the *f* electrons—the stronger the dispersion, the farther the peak shifts—and the width reflects the damping of the *f* electrons—the larger the damping, the wider the peak. Besides, the temperature behavior of the peak is controlled by both the spectral function and the Fermi profile.

As pointed out in the preceding section, $J_1 s$ is much less than the *c*-electron bandwidth, therefore, $\xi_{\mathbf{k}}=-2J_1 s[\cos(k_x a)+\cos(k_y a)+\cos(k_z a)]$ will vary slowly when $\mathbf{k}$ scans through the Brillouin zone, as a consequence, the Lorentzian peak as well as the ARPES peak can move only quite a small distance when $\mathbf{k}$ scans from (π,π,π), the bottom of the band, to $(0,0,0)$, the top of the band, which can be seen directly from Fig. 6, and

$$\Pi(\mathbf{k},\omega) \propto \frac{\Gamma_f}{(\omega'-\{\varepsilon_f-2J_1 s[\cos(k_x a)+\cos(k_y a)+\cos(k_z a)]\})^2+\Gamma_f^2} f(\omega'-\mu). \tag{77}$$

The numerical results of the ARPES are depicted in Fig. 8, with the bandwidth of the bare *c* electrons supposed to be 6 eV. The shift of the ARPES peak is about 40 meV when $\mathbf{k}$ scans from the bottom of the band to the top of the band, such a small shift of the peak is a reflection of the weak dispersion of the *f*-electron band, which is qualitatively in agreement with the experiments where the observed shift is about 20–35 meV for different samples.[2–4] In addition, as both the hopping amplitude *s* and the damping Γ_f depend weakly on temperature, Eq. (77) indicates that the Lorentzian peak will depend on temperature weakly, as has been shown in Fig. 7. Thereby, the temperature behavior of the ARPES

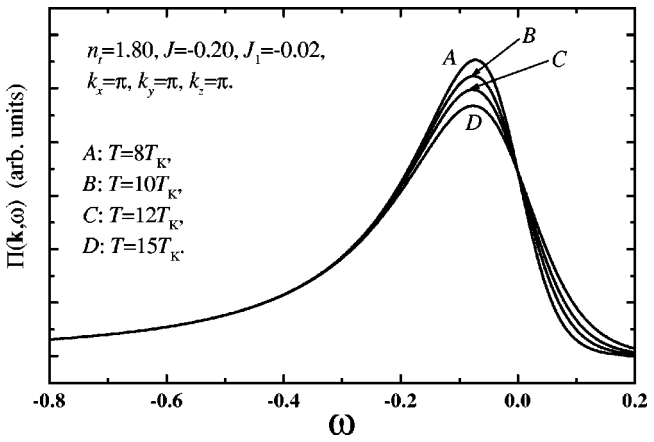

FIG. 9. The temperature dependence of the *f*-electron ARPES.

arises mainly from the Fermi profile, which means that the ARPES will be weakly temperature dependent because the Fermi profile is weakly temperature dependent in the experimental temperature range. This is depicted in Fig. 9, which shows that the theoretical result is in accordance with the experiments.[2–4] Compared with the PAM,[8,9] the *f*-electron ARPES is now both of weak dispersion and of weak temperature dependence at $T \gg T_K$ within the EKLM, whereas it is only weakly temperature dependent but strongly dispersive in the PAM.

On all accounts, the extended Kondo lattice model is able to interpret theoretically both the weak dispersion and weak temperature dependence of the ARPES of the *f* electrons observed experimentally.

VI. SUMMARY AND CONCLUSIONS

After including an exchange term between the *c* and *f* electrons on nearest-neighbor sites, we have developed an extended Kondo lattice model, and used it to explain the weak dispersion and weak temperature behaviors of the angle-resolved photoemission spectroscopies of the *f* electrons at $T \gg T_K$. It is found that the extended Kondo lattice model just produces a small renormalization to the low-temperature coherence when compared with the Kondo lattice model, namely, it maintains the low-temperature coherence of heavy-fermion systems, which is fundamental to comprehend the low-temperature properties of those systems. Unlike the Kondo lattice model, the extended Kondo lattice model causes the *f* electrons to build a narrow itinerant band at $T \gg T_K$, and contributes an angle-resolved photoemission peak with weak dispersion and weak temperature dependence to the *f* electrons, which is in agreement with the experiments. In other words, the extended Kondo lattice model can account for both the low-temperature coherence and the *f*-electron ARPES in the high-temperature range.

In this paper, we have just used the EKLM to discuss the ARPES of the nonmagnetic heavy-fermion systems. In principle, it can also be applied to the magnetic systems, which is under consideration.

ACKNOWLEDGMENTS

This work was supported by the State Key Project of Fundamental Research under Grant No. 001CB610602.

[1] For a review, see D.W. Hess, P.S. Riseborough, and J.L. Smith, in *Encyclopedia of Applied Physics*, edited by G.L. Trigg (VCH, New York, 1991), Vol. 7, p. 435; N. Grewe and F. Steglich, in *Handbook on Physics and Chemistry of Rare Earths*, edited by K.A. Gschneidner, Jr. and L.L. Eyring (Elsevier, Amsterdam, 1991), Vol. 14, p. 343.

[2] A.B. Andrews, J.J. Joyce, A.J. Arko, J.D. Thompson, J. Tang, J.M. Lawrence, and J.C. Hemminger, Phys. Rev. B **51**, 3277 (1995).

[3] A.B. Andrews, J.J. Joyce, A.J. Arko, Z. Fisk, and P.S. Riseborough, Phys. Rev. B **53**, 3317 (1996).

[4] A.J. Arko, J.J. Joyce, A.B. Andrews, J.D. Thompson, J.L. Smith, D. Mandrus, M.F. Hundley, A.L. Cornelius, E. Moshopoulou, Z. Fisk, P.C. Canfield, and A. Menovsky, Phys. Rev. B **56**, R7041 (1997).

[5] C. Lacroix, and M. Cyrot, Phys. Rev. B **20**, 1969 (1979).

[6] D.M. Newns, and N. Read, Adv. Phys. **36**, 799 (1987).

[7] Z.Z. Li, M. Zhuang, and M.W. Xiao, J. Phys.: Condens. Matter **8**, 7941 (1996).

[8] A.N. Tahvildar-Zadeh, M. Jarrell, and J.K. Freericks, Phys. Rev. Lett. **80**, 5168 (1998).

[9] Ming-wen Xiao and Zhen-zhong Li, Solid State Commun. **118**, 63 (2000).

[10] T. Kasuya, Prog. Theor. Phys. **16**, 45 (1956).

[11] N. Andrei, Phys. Rev. Lett. **45**, 379 (1980).

[12] D.N. Zuberev, *Nonequilibrium Statistical Thermodynamics* (Consultants Bureau, New York, 1974), Chap. 3.

[13] A.A. Abrikosov, Physics (Long Island City, N.Y.) **2**, 5 (1965).

[14] B. Schuh, Z. Phys. B **34**, 37 (1979).

[15] Z.Z. Li, Q.Q. Zheng, and Y.L. Liu, Commun. Theor. Phys. **1**, 273 (1982).

[16] P.W. Anderson, Phys. Rev. **124**, 41 (1961).

[17] M.W. Xiao, and Z.Z. Li, Phys. Rev. B **49**, 13 160 (1994).

[18] M.W. Xiao, and Z.Z. Li, Commun. Theor. Phys. **23**, 257 (1995).

[19] D.N. Shi, M.W. Xiao, and Z.Z. Li, Physica C **282**, 1673 (1997).

[20] D.N. Shi, M.W. Xiao, and Z.Z. Li, Phys. Rev. B **58**, 12 478 (1998).